Interactions of Carbon-Nanotubule Proximal Probe Tips with Diamond and Graphene

Ajay Garg,[1] Jie Han,[2] and Susan B. Sinnott[1]
[1]*Department of Chemical and Materials Engineering, The University of Kentucky, Lexington, Kentucky 40506-0046*
[2]*NASA Ames Research Center, Moffett Field, California 94035-1000*
(Received 18 February 1998)

Interactions between proximal probe tips composed of carbon nanotubules (CNTs) and diamond and graphene surfaces are investigated using molecular dynamics simulations. The simulations reveal the mechanisms of buckling, bending, slipping, and elastic recovery of the CNT tips on these surfaces and suggest that they will not wear out when crashed as conventional tips often do unless the surface is highly reactive. The simulations also show how the deformation mechanism changes as a function of tubule length and the effect of these changes on the buckling force is discussed quantitatively. [S0031-9007(98)07108-7]

PACS numbers: 61.16.Ch, 61.48.+c

The last two decades have seen phenomenal changes in the field of nanotechnology. Specifically, powerful new methods have been developed to investigate and manipulate matter on the nanometer scale with proximal probes, such as the scanning tunneling microscope (STM) [1], the atomic-force microscope (AFM) [2], and related methods. The STM has been used to image surfaces, build nanometer-scale structures, and pattern surfaces in an atom-by-atom fashion through a voltage between the tip and the sample [3]. Best images are obtained for atomically sharp STM tips and both sample and tip must be conducting. In contrast, the AFM measures the mechanical forces between a tip that is attached to a stiff cantilever and a surface. It has been used to investigate the nanometer-scale mechanical properties of materials [4] and atomic-scale friction [5].

Concurrently, novel nanometer-scale materials, carbon nanotubes (CNTs), were discovered and extensively studied. Nanotubes are classified according to the helical symmetry around the axis of the cylinder, denoted by two integers, (m, n), that indicate the number of lattice vectors in the graphite plane used to make the tubule [6]. There are only two, high-symmetry, achiral nanotubules, "zigzag" $(m, 0)$ and "armchair" (m, m). It has been shown that small-diameter zigzag nanotubules are semiconducting while small-diameter armchair tubules are metallic [7,8]. In addition, calculations [9–12] and experiments [13] indicate that nanotubules have high strength in the direction of the tubule axis, with a calculated or measured Young's moduli of 1–5 TPa.

Smalley and co-workers [14] have recently used a CNT as a proximal probe tip by attaching it with adhesive to the tip of a conventional silicon cantilever. This CNT, which was about 2 μm long with a radius of 0.68 nm, was shown to provide increased resolution over traditional Pt/W tips that are typically 1–100 nm in size at the apex. The Euler buckling force was calculated to be 5 nN assuming a Young's modulus of 1 TPa. Molecular dynamics simulations have also investigated the mechanical interactions of capped $(10, 10)$ CNTs with diamond surfaces and shown how the cap flattens and inverts when pressed against hydrogen-terminated diamond (111) [15].

In this Letter we investigate the effects of nanotubule length and surface type on the mechanisms of the interaction of carbon nanotubules with surfaces. The surfaces considered are hydrogen-terminated, diamond (111), C(111):H, the (1×1) non-hydrogen-terminated diamond (111) surface, C(111):C, and a graphene sheet. Capped $(10, 10)$ CNT tips with lengths of 5.0, 8.1, and 13.4 nm are considered. Throughout the simulations, 100 atoms at the tubule ends farthest from the surface are held fixed (i.e., they are not allowed to evolve in time) to mimic the rigid cantilever used in the experiments [14] following the example of Landman *et al.* [4]. We calculate the force on the fixed atoms due to indentation in a manner that is comparable to the experimental measurement of force with a rigid cantilever. Moving towards the center of the tubules, the next 200 atoms had Langevin thermostats applied to maintain the temperature of the system at 300 K. The remaining atoms evolved in time according to Newton's equations of motion with no constraints.

The simulations use a reactive, empirical bond-order potential for hydrocarbons of the Abell-Tersoff formalism that was parameterized by Brenner [16,17]. They were carried out at a constant temperature of 300 K with a time step of 0.15 fs.

The indentation process proceeded as follows: The tip started off about 0.2 nm above the surface and moved towards the surface in increments of 0.005 nm. When the tip displacement relative to the surface becomes larger than the initial spacing between the tip and the surface of 0.2 nm, the tip is compressed against the surface. The entire system was allowed to equilibrate for 400 time steps in between displacements of the tip, and the forces on the tip due to the indentation were averaged over the last 100 of these 400 steps. Additional averaging was performed on the force-displacement curves to filter out the noise

 0031-9007/98/81(11)/2260(4)$15.00

from thermal vibrations. These conditions are similar to those previously used to model the indentation of C(111):H with a square-pyramidal, hydrogen-terminated diamond asperity tip [18] and a comparison to those results is made below.

The first series of simulations considered the indentation of the C(111):H surface with the capped (10, 10) nanotubule tips and Fig. 1 shows selected snapshots from some of these simulations. As the CNT's were pushed against the surface, the caps are flattened and then inverted, behavior identical to that reported in Ref. [15]. As the tips continue to push against the surface, kinks or buckles develop in the body of the tubules that correspond to modulations in the force curve shown in Fig. 2. The shortest CNT tip experiences a single buckle while the longer tubules each develop two well-defined buckles or kinks. By the time the tips have been pushed 0.6–0.8 nm against the surface, they abruptly "slip" such that the tubules are sharply bent with the ends pointing up, as shown in Fig. 1(b). This corresponds to the large drop in the force in Fig. 2.

The maximum force felt by all three CNT's occurs prior to the development of the kinks at about 80 nN and the average slopes of the force curves were around 2 nN/A. In general, longer tubules were able to press farther against the surface before slipping and bending than shorter tubules. On retraction, the tubules returned to their original configurations and the diamond surface does not show any deformation as a result of being indented.

Hence these indentations are fully elastic. This is in contrast to the results obtained with diamond asperity tips [18] indenting C(111):H, where the tips deformed through twist and shear mechanisms up to an indentation depth of about 0.5 nm (maximum force of about 200 nN) before bonds within the tips began to break. This resulted in adhesion between the tips and the surface not seen in the simulations with the CNT tips. Hence the tubules are shown to be able to withstand failure when crashed or pressed against unreactive, rigid surfaces due to their ability to buckle, bend, and slip to reliever applied stress, rather than build up stress and then fracture in a brittle fashion like diamond. When capped CNT's indented the reactive C(111):C surface, however, the results were quite different. Adhesion occurred between the CNT and the surface on contact due to the highly reactive nature of this surface. As a consequence, the CNT was destroyed on withdrawal as shown in Fig. 3.

Finally, we consider the result of indenting capped CNT tips against a surface that is compliant and easily deformed, such as a graphene sheet. As the CNT tips indent the graphene, the sheet deforms so that the tips are pushed against the surface for 1.5 nm (2.0 nm for the longest tubule tip considered) before buckling and slipping at a maximum buckling force of about 100 nN [see Fig. 4(a)]. Again, the shortest CNT tip buckles only once whereas the longer tubules each buckle twice before slipping [see Fig. 4(b)]. On retraction, both the CNT tips and the graphene sheet return to their original configurations.

The combined flexibility of the CNT's and the graphene leads to a small average slope of 1 nN/A for the force curve. The larger buckling force is due to the fact that the deformation of the graphene prevents the CNT from slipping as readily as it was able to do on the diamond surface.

Thus, the mechanism of CNT tip deformation during the indentation processes does not depend on the rigidity of the surface. However, the number of buckles induced in the CNT tips as they contact a solid surface does depend on the tube length. To try to better understand this phenomenon, additional simulations were performed where the CNT's of varying lengths were compressed by holding both ends fixed and moving one end towards the other as was done during the indentation. The buckling force, number of buckles, and Young's modulus can be

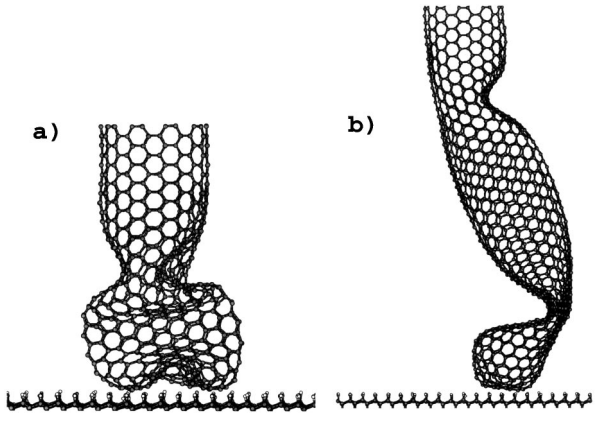

FIG. 1. Snapshots from simulations where capped CNT tips indented C(111):H surfaces. (a) Buckling and cap inversion for a 5.0-nm-long CNT tip, and (b) two buckles with some slip for a 8.1-nm-long CNT tip.

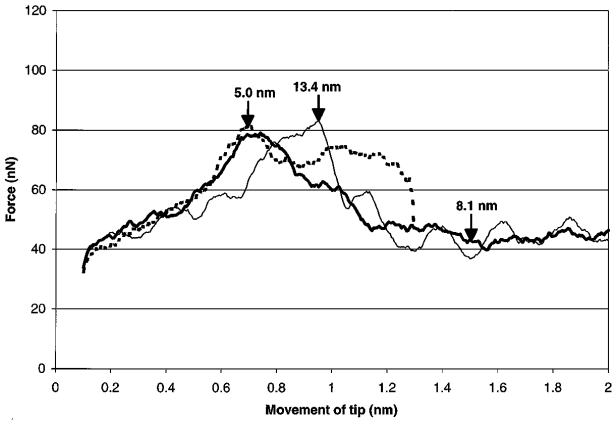

FIG. 2. Force-distance curves for capped CNT tips indenting C(111):H surfaces.

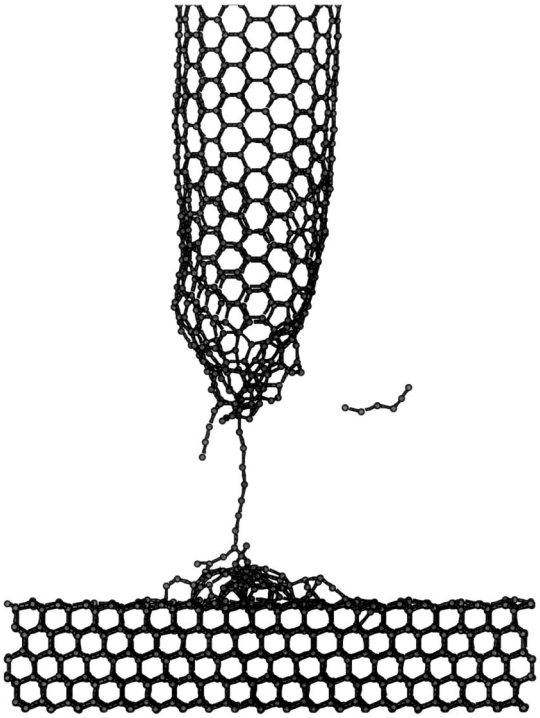

FIG. 3. Snapshot from a simulation where a capped 8.1-nm-long CNT tip indented and adhered to a C(111):C surface.

correlated by the following classical mechanics equation for buckling of a column [19]

$$M = Fd\sin[(n\pi x)/L], \qquad n = 1, 2, 3, \ldots, \qquad (1)$$

where M is the bending moment, F is force experienced by the column, d is a maximum deflection, L is the column length, and n is the number of buckles. The solution to Eq. (1) at the maximum deflection can be simplified to

$$F = YI(n\pi/L)^2, \qquad (2)$$

where Y is the Young's modulus and I is the stress moment over the cross section of the nanotubule radius ($I \approx \pi r^4/4$). This corresponds to the Euler buckling force when there is only one buckle ($n = 1$):

$$F_{\text{EULER}} = (\pi^2 YI)/L^2. \qquad (3)$$

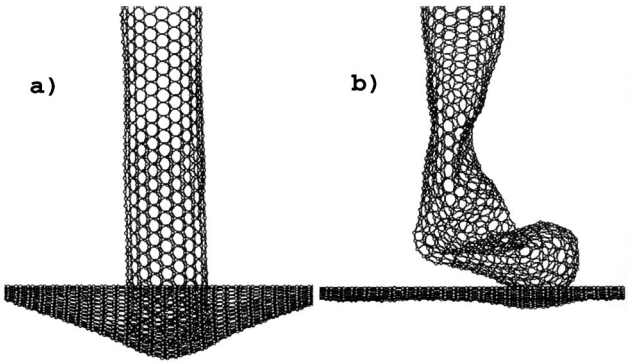

FIG. 4. Snapshots from simulations where capped CNT tips indented graphene sheets. (a) Deformation of the sheet as a capped 8.1-nm-long CNT tip presses against it, and (b) the tip has buckled and slipped.

Equation (2) was used to calculate the Young's moduli of (10, 10) tubules as function of tubule length, number of buckles, and applied force determined from the simulations. The results are presented in Table I.

Examination of the table shows the magnitude of the buckling force is strongly dependent on the degrees of freedom available to the end of the CNT tip. When the CNT tip indented C(111):H, the interactions between the tip and surface were highly repulsive and the tip was able to deform several different ways in addition to buckling, such as through cap inversion and slip. This resulted in lower overall buckling forces. In the free space compressions, the ends of the CNT are fixed, thus removing the strain-reduction mechanisms of cap inversion and slip. Therefore, the buckling force for a CNT compressed in space is higher than that seen during surface indentation.

Table I also shows that Eq. (2), which takes into account the number of buckles, provides quite reasonable and consistent moduli when buckling is the only mechanism available to reliever strain (i.e., the free-space compression cases). Close examination of the simulation results for the longest CNT tip indentation on C(111):H reveals that before the body of the tubule can develop a third buckle, the end of the tip has experienced sufficient repulsion with the surface to cause the end to slip. Hence, tubules that will buckle several times when

TABLE I. Dependence of the buckling force obtained from the indentation and compression simulations and the Young's modulus calculated with Eq. (2) on the tubules' available degrees for freedom and length. Indentation results are for the C(111):H surface.

	# Buckles		Buckling Force (nN)		Modulus (TPa)	
CNT Length (nm)	Indent	Free Space	Indent	Free Space	Indent	Free Space
5.0	1	1	82	85	1.2	1.3
7.3	···	2	···	100	···	0.8
8.1	2	2	79	110	0.8	1.0
12.3	···	3	···	130	···	1.3
13.4	2	3	85	120	2.3	1.4

compressed in space, may not necessarily do so when indented against a surface due to slip. There are fluctuations in the forces and moduli that cannot be explained by changes in the tubule length alone. These are due to thermal noise and the averaging of the raw force data from the simulations. It is recognized that the modulus of the (10, 10) tubule is in reality a constant, and the average value obtained from the free-space compressions is 1.2 TPa, in excellent agreement with the most recent calculations [20].

In Ref. [14], Eq. (3) was used to obtain the buckling force of 5 nN for the 2 μm (10, 10) tubule, where the Young's modulus was assumed to be 1 TPa. These simulations show that the actual buckling force is much higher, but to determine the true value, the number of buckles or kinks in the CNT tip would have to be included in the calculation, as shown in Eq. (2). In addition, the simulations indicate that there were most likely other deformation mechanisms at work during the experimental indentation, such as gap inversion and slip.

In conclusion, our simulations indicate that nanotubules make ideal proximal probe tips because they do not plastically deform during tip crashes on unreactive surfaces as conventional tips often do. Instead, they elastically deform, buckle and slip, mechanisms that would have to be taken into account if CNT tips were used in an AFM. However, in the case of highly reactive surfaces strong adhesion can occur between the CNT and the surface that destroys the CNT. Finally, we wish to point out that recent experimental data for the indentation of CNT tips on H-terminated Si surfaces [21] finds a Young's modulus of 1.2 TPa for the (10, 10) tubule and confirms the mechanisms revealed by this simulation work of buckling-slipping-bending-recovering.

The authors gratefully acknowledge the support of NASA Ames Research Center (Grant No. NAG2-1121).

[1] G. Binnig and H. Rohrer, Helv. Phys. Acta **55**, 762 (1982).
[2] G. Binnig, C. F. Quate, and Ch. Gerber, Phys. Rev. Lett. **56**, 930 (1986).
[3] D. M. Eigler, C. P. Lutz, and W. E. Rudge, Nature (London) **352**, 600 (1991).
[4] U. Landman *et al.*, Science **248**, 454 (1990).
[5] C. M. Mate *et al.*, Phys. Rev. Lett. **59**, 1942 (1987).
[6] M. S. Dresselhaus, G. Dresselhaus, and P. C. Eklund, *Science of Fullerenes and Carbon Nanotubules* (Academic Press, San Diego, 1996).
[7] J. W. Mintmire, B. I. Dunlap, and C. T. White, Phys. Rev. Lett. **68**, 631 (1992).
[8] S. J. Tans et al., Nature (London) **386**, 474 (1997).
[9] D. H. Robertson, D. W. Brenner, and J. W. Mintmire, Phys. Rev. B **45**, 12 592 (1992).
[10] B. I. Yakobson, C. J. Brabec, and J. Bernholc, Phys. Rev. Lett. **76**, 2511 (1996).
[11] C. F. Cornwell and L. T. Wille, Solid State Commun. **101**, 555 (1997).
[12] S. B. Sinnott *et al.*, Carbon **36**, 1 (1998).
[13] M. M. J. Treacy, T. W. Ebbesen, and J. M. Gibson, Nature (London) **381**, 678 (1996).
[14] H. Dai *et al.*, Nature (London) **384**, 147 (1996).
[15] J. A. Harrison *et al.*, J. Phys. Chem. B **101**, 9682 (1997).
[16] D. W. Brenner, Phys. Rev. B **42**, 9458 (1990).
[17] D. W. Brenner, S. B. Sinnott, O. A. Shenderova, and J. A. Harrison (unpublished).
[18] S. B. Sinnott *et al.*, J. Vac. Sci. Technol. A **15**, 936 (1997).
[19] D. O. Brush and B. Almroth, *Buckling of Bars, Plates, and Shells* (McGraw-Hill, New York, 1975).
[20] J. P. Lu, Phys. Rev. Lett. **79**, 1297 (1997).
[21] H. Dai, N. Franklin, and J. Han, (to be published).